. Capability of Energy Storage System based Supplementary Damping Control to Suppress Power System Inter-area Oscillations

Wang, H. (2011). . Capability of Energy Storage System based Supplementary Damping Control to Suppress Power System Inter-area Oscillations. IET Generation, Transmission and Distribution, 0.

Published in:
IET Generation, Transmission and Distribution

Capability of Energy Storage System based Supplementary Damping Control to Suppress Power System Inter-area Oscillations

W. Du, H. F. Wang *(SMIEEE)*, J. Cao and L Xiao

***Abstract* – In order to understand how an energy storage system (ESS) based supplementary damping control (stabilizer) suppresses power system inter-area oscillations, this paper proposes a tie-line power variation related ESS linearized dynamic model. This model describes the direct contribution from the ESS control to the small-signal variations (oscillations) of the tie-line power. Based on the model, a general conclusion is established to assess the capability of the ESS based stabilizer to affect the damping of inter-area power oscillation. Analysis based on the general conclusion explains why the robustness of the ESS stabilizer to the variations of tie-line loading level is different when it is implemented by regulating either active or reactive power exchange between the ESS and the power system. A new method to design the ESS stabilizer is developed from the tie-line power variation related ESS linearized dynamic model and the established general conclusion. The design is simple and localized because it relies only on the proposed tie-line power variation related ESS linearized model without the need to be referred to a mathematical model of whole power system. In the paper, results of computation and simulation of an example power system installed with a battery energy storage system (BESS) are presented.**

Index Terms **- energy storage system (ESS), battery ESS, inter-area power system oscillations.**

I. Introduction

An energy storage system (ESS) can function not only by regulating its reactive power exchange with a power system as a FACTS controller does, but also through directly injecting or absorbing active power into or from the power system instantaneously. Hence the ESS is considered to have significant potential to improve power system stability, including to enhance the damping of power system oscillations. There are four types of ESSs which can assist power system dynamic operation. They are superconducting magnetic energy storage systems (SMES), battery energy storage systems (BESS), advanced super-capacitors (ASC) and flywheel energy storage systems (FESS) [1].

Capability of SMES based supplementary damping control to suppress power system oscillations has been well demonstrated via modal computation, simulation, experiment and field tests [2]-[6]. Integrated use of FACTS controllers and ESS units to improve power system oscillation stability has also been investigated. It is now well accepted that addition of ESS units can provide the FACTS controllers extra ability of active power modulation such that better control performance can be achieved [7]-[9]. BESS based stabilizer (BESS PSS) has been demonstrated by field tests [10]. Though there have not been many publications on the FESS and ASC based stabilizers, it can be expected that they should be able to function as effectively as the SMES and BESS stabilizers if their applications in power systems are cost-effectively feasible in future.

This paper studies the capability of an ESS based stabilizer to suppress power system inter-area oscillation. The focus of discussion is to understand how the ESS stabilizer provides damping to inter-area power oscillation. In order for the discussion to cover four main types of ESSs, it is considered in the paper that the ESS is connected to a multi-machine power system through a DC/AC voltage source converter (VSC). The paper considers two types VSC control schemes for grid connection, the pulse width modulation (PWM) and the pulse amplitude modulation (PAM). A tie-line power variation related ESS linearized dynamic model (TPVELDM) is proposed in the paper to show the contribution from the ESS to the small-signal variation (oscillation) of tie-line power. A general conclusion on how the ESS based stabilizer affects the damping of power system inter-area oscillation is established by using the linearized equal area criterion. Based on the TPVELDM and the general conclusion established, a method for the design of the ESS based stabilizer is proposed. This method is simple because stabilizer design is carried out by use of the localized TPVELDM without the need to be referred to a mathematical model of the whole power system. In the paper, robustness of the ESS based stabilizer to the variations of tie-line loading level is examined. It is concluded that the ESS based stabilizer through directly regulating the exchange of active power is more robust. An example power system installed with a BESS based stabilizer is presented.

II. Tie-line Power Variation Related ESS Linearized Dynamic Model

Figure 1 shows an ESS installed at a node along a tie line from node A to B in a multi-machine power system. The ESS is of a two stage configuration of power electronics for grid

W. Du is with the Southeast University, Nanjing China, and working at the Queen's University of Belfast, Belfast, UK, at present (e-mail: ddwenjuan@googlemail.com). Prof. H F Wang and Mr. J Cao are with the Queen's University of Belfast, Belfast, UK. Prof. L Xiao is with the Institute of Electrical Engineering, Chinese Academy of Sciences, China.

connection which is commonly used for the SMES and BESS [11]. The second converter is for enhancing or regulating the output from the energy storage unit, i.e., the battery or superconducting coil. This two stage grid connection can also be employed by the FESS, where the second converter is a AC/DC converter [12]. Obviously without the second converter ($I_{dc2}=0$), it can be a single-stage configuration for the ASC and BESS. Hence the two-stage configuration can represent the main four types of ESSs.

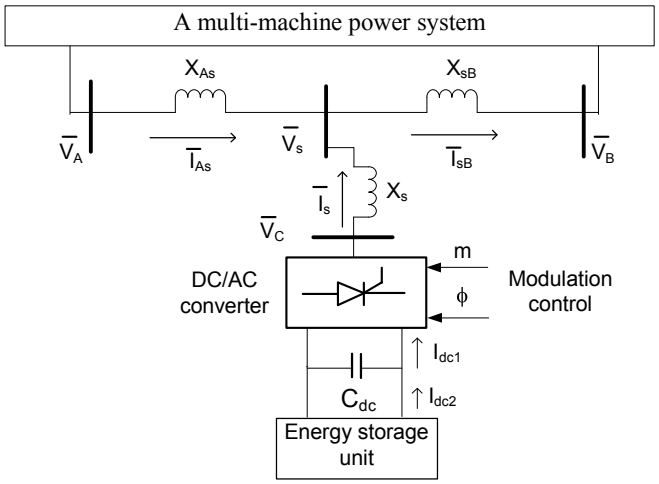

Figure 1 An ESS installed in a multi-machine power system

Voltage at the ac terminal of the DC/AC converter is [11]

$$\bar{V}_C = mkV_{dc}\angle\gamma = mkV_{dc}\angle\varphi+\phi \tag{1}$$

where k is a constant dependent of the structure of the DC/AC converter, V_{dc} the dc voltage at the dc terminal of the DC/AC converter. Modulation phase, ϕ , is the phase difference between $\bar{V}_C = V_C\angle\gamma$ and $\bar{V}_S = V_S\angle\varphi$, i.e, $\phi=\gamma-\varphi$. If the DC/AC converter is controlled by the pulse width modulation (PWM) control, m and ϕ is the modulation ration and phase of the PWM respectively. If the control algorithm of the DC/AC converter is the pulse amplitude modulation (PAM), $m=1$.

The active power exchange between the ESS and power system is

$$V_{dc}I_{dc1} = I_{sd}V_{cd}+I_{sq}V_{cq} = I_{sd}mkV_{dc}\cos\phi+I_{sq}mkV_{dc}\sin\phi$$

where subscript d and q denotes the d and q component of the corresponding variable respectively in the d-q coordinate of the ESS as shown by Figure 2. Hence

$$\begin{aligned}\dot{V}_{dc} &= \frac{1}{C_{dc}}(-I_{dc1}+I_{dc2})\\ &= \frac{1}{C_{dc}}(-I_{sd}mk\cos\phi-I_{sq}mk\sin\phi+I_{dc2})\end{aligned} \tag{2}$$

Linearization of Eq.(2) is (see Appendix 1)

$$s\Delta V_{dc} = -k_{dc}\Delta\phi+\frac{\Delta I_{dc2}}{C_{dc}} \tag{3}$$

where k_{dc} is a constant.

There have been various current, voltage or/and power control based schemes proposed so far to implement the PWM or PAM for the DC/AC converter [11][13]-[15]. Without the loss of generality of discussion and affecting the demonstration to develop a tie-line power variation related ESS linearized dynamic model (TPVELDM), the following AC and DC voltage based control functions are considered for the PWM algorithm [11]

$$m = m_0+K_{ac}(s)(V_{sref}-V_s)+u_{pss-m} \tag{4}$$

$$\phi = \phi_0+K_{dc}(s)(V_{dcref}-V_{dc})+u_{pss-f} \tag{5}$$

where $K_{ac}(s)$, $K_{dc}(s)$ is the transfer function of AC and DC voltage controller of the DC/AC converter; u_{pss-m} and u_{pss-f} is the supplementary damping control signal superimposed on the AC and DC voltage control function respectively. Because the ESS supplementary damping controller associated with u_{pss-m} and u_{pss-f} is implemented through regulating the exchange of reactive and active power between the ESS and the power system, it is named as ESS reactive power PSS (power system stabilizer) and active power PSS in this paper.

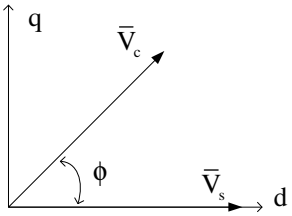

Figure 2 Phasor diagram in the d-q coordinate of the ESS

Voltage based control scheme to implement the PAM algorithm for the DC/AC converter is [11]

$$\phi = \phi_0+K_1(s)[\frac{1}{k}K_2(s)(V_{sref}-V_s+u_{pss-pam})+\frac{1}{k}V_{sref}-V_{dc}] \tag{6}$$

where $u_{pss-pam}$ is the supplementary damping control signal; $K_1(s)$ and $K_2(s)$ the transfer function of two controllers.

From Appendix 2, linearization of Eq.(4)-(6) can be obtained to be

$$\begin{aligned}\Delta m &= -\frac{K_{ac}(s)(h_1\Delta V_{dc}+h_3\Delta\phi+h_4\Delta\delta_{AB}+h_5\Delta V_A+h_6\Delta V_B)}{1+h_2K_{ac}(s)}\\ &+\frac{1}{1+h_2K_{ac}(s)}\Delta u_{pss-m}\\ \Delta\phi &= -K_{dc}(s)\Delta V_{dc}+\Delta u_{pss-f}\end{aligned} \tag{7}$$

$$\begin{aligned}\Delta\phi &= \frac{-K_1(s)K_2(s)(h_4\Delta\delta_{AB}+h_5\Delta V_A+h_6\Delta V_B)}{k+h_3K_1(s)K_2(s)}\\ &+\frac{K_1(s)K_2(s)}{k+h_3K_1(s)K_2(s)}\Delta u_{pss-pam}-\frac{K_1(s)K_2(s)h_1+kK_1(s)}{k+h_3K_1(s)K_2(s)}\Delta V_{dc}\end{aligned} \tag{8}$$

From Figure 1 it can have

$$\begin{aligned}\bar{V}_S &= jX_{sB}\bar{I}_{sB}+\bar{V}_B = jX_{sB}[\bar{I}_{As}-(\frac{\bar{V}_S-\bar{V}_C}{jX_S})]+\bar{V}_B\\ &= jX_{sB}\bar{I}_{As}-\frac{X_{sB}}{X_S}\bar{V}_S+\frac{X_{sB}}{X_S}\bar{V}_C+\bar{V}_B\end{aligned} \tag{9}$$

That gives

$$\bar{V}_S = \frac{jX_{sB}}{1+\frac{X_{sB}}{X_S}}\bar{I}_{As} + \frac{X_{sB}}{X_S(1+\frac{X_{sB}}{X_S})}\bar{V}_C + \frac{\bar{V}_B}{1+\frac{X_{sB}}{X_S}} \tag{10}$$

Hence it can be obtained that

$$\bar{V}_A = jX_{As}\bar{I}_{As} + \bar{V}_S = j(X_{As} + \frac{X_S X_{sB}}{X_S + X_{sB}})\bar{I}_{As}$$
$$+ \frac{X_{sB}}{X_S + X_{sB}}\bar{V}_C + \frac{X_S}{X_S + X_{sB}}\bar{V}_B \tag{11}$$
$$= jX\bar{I}_{As} + \bar{V}_a$$

where

$$X = (X_{As} + \frac{X_S X_{sB}}{X_S + X_{sB}}),$$

$$\bar{V}_a = \frac{X_{sB}}{X_S + X_{sB}}\bar{V}_C + \frac{X_S}{X_S + X_{sB}}\bar{V}_B = a\bar{V}_C + b\bar{V}_B$$

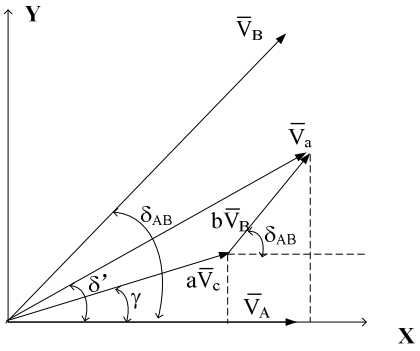

Figure 3 Phasor diagram in the X-Y coordinate of the power system

From Eq.(11) and the phasor diagram of Figure 3, the active power delivered from node A along the transmission line can be obtained to be

$$P_A = \frac{V_a V_A}{X}\sin\delta' = \frac{V_A}{X}(bV_B\sin\delta_{AB} + akmV_{dc}\sin\gamma)$$
$$= \frac{V_A}{X}bV_B\sin\delta_{AB} + \frac{V_A}{X}akmV_{dc}\sin(\varphi+\phi) \tag{12}$$

Hence small-signal variation of tie line power is

$$\Delta P_A = \frac{\partial P_A}{\partial \delta_{AB}}\Delta\delta_{AB} + \frac{\partial P_A}{\partial V_A}\Delta V_A + \frac{\partial P_A}{\partial V_B}\Delta V_B + \frac{\partial P_A}{\partial \varphi}\Delta\varphi$$
$$+ \frac{\partial P_A}{\partial V_{dc}}\Delta V_{dc} + \frac{\partial P_A}{\partial m}\Delta m + \frac{\partial P_A}{\partial \phi}\Delta\phi \tag{13}$$

Obviously Eq.(13) can be denoted as

$$\Delta P_A = \frac{\partial F(\mathbf{z},\mathbf{u}_{ess})}{\partial \mathbf{z}}\Delta\mathbf{z} + \frac{\partial F(\mathbf{z},\mathbf{u}_{ess})}{\partial u_{pss}}\Delta\mathbf{u}_{ess}$$
$$= \Delta P_A(\Delta\mathbf{z}) + \Delta P_A(\Delta\mathbf{u}_{ess}) \tag{14}$$

where

$\mathbf{z} = [\Delta\delta_{AB} \quad \Delta V_A \quad \Delta V_B \quad \Delta\varphi]^T$, $\mathbf{u}_{ess} = [\Delta V_{dc} \quad \Delta m \quad \Delta\phi]^T$ and $\Delta P_A(\Delta\mathbf{u}_{ess})$ is the direct contribution from the ESS to the variation of tie line power. From Eq.(12) and (14) it can have

$$\Delta P_A(\Delta\mathbf{u}_{ess}) = F_{dc}\Delta V_{dc} + F_m\Delta m + F_f\Delta\phi \tag{15}$$

where

$$F_{dc} = \frac{V_A}{X}akm_0\sin\gamma_0, F_m = \frac{V_A}{X}akV_{dc0}\sin\gamma_0,$$
$$F_f = \frac{V_A}{X}akm_0V_{dc0}\cos\gamma_0$$

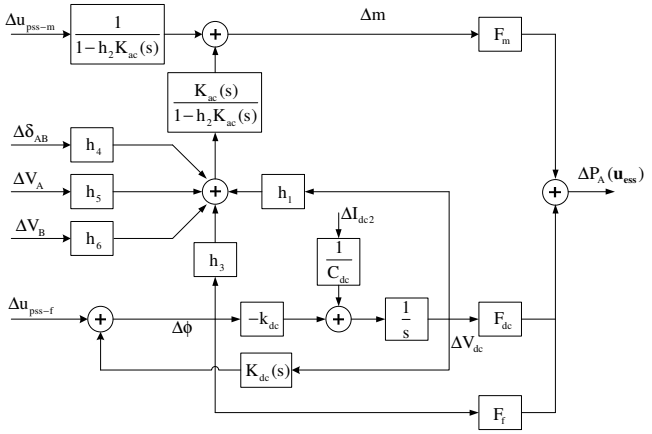

Figure 4 Tie-line power variation related ESS linearized dynamic model when the PWM is used

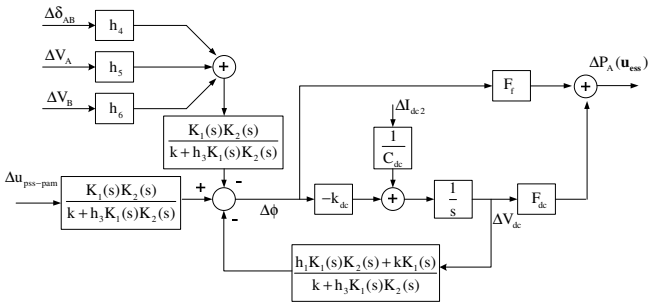

Figure 5 Tie-line power variation related ESS linearized dynamic model when the PAM is used

Figure 4 is constructed by using Eq.(3), (6), (7) and (15), showing the ESS direct contribution to the variation of tie-line power when the PWM control is implemented by the DC/AC converter. Figure 5 is built from Eq.(3), (8) and (15) about the ESS direct contribution to the variation of tie-line power when the PAM control is used for the DC/AC converter ($\Delta m = 0, C_m = 0$). They are named as the tie-line power variation related ESS linearized dynamic model (TPVELDM). It is used to examine how an ESS based stabilizer provides damping to suppress the tie-line (inter-area) power oscillation (variation) in the following section.

III. Capability of ESS based stabilizers to damp inter-area power oscillations

According to the superimposition principle of linear systems, from Figure 4 and 5 it can have

$$\Delta P_A(\Delta\mathbf{u}_{ess}) = \Delta P_{A-ess}(\Delta\mathbf{z}) + \Delta P_A(\Delta I_{dc2})$$
$$+\Delta P_A(\Delta u_{pss-m}) + \Delta P_A(\Delta u_{pss-f}) \tag{16}$$

$$\Delta P_A(\Delta\mathbf{u}_{ess}) = \Delta P_{A-ess}(\Delta\mathbf{z}) + \Delta P_A(\Delta I_{dc2})$$
$$+\Delta P_A(\Delta u_{pss-pam}) \tag{17}$$

where $\Delta P_{A-ess}(\Delta \mathbf{z})$, $\Delta P_A(\Delta I_{dc2})$, $\Delta P_A(\Delta u_{pss-m})$, $\Delta P_A(\Delta u_{pss-f})$ and $\Delta P_A(\Delta u_{pss-pam})$ is the direct contribution to $\Delta P_A(\Delta \mathbf{u}_{ess})$ from $\Delta \mathbf{z}$, ΔI_{dc2} , Δu_{pss-m} , Δu_{pss-f} and $\Delta u_{pss-pam}$ respectively. Direct damping contribution to the tie line power oscillation from an ESS based stabilizer can be examined by using the following general conclusion.

Conclusion: D*ecomposition of direct contribution from the ESS based stabilizer to the variation of tie line power in* $\Delta\delta_{AB} - \Delta\dot{\delta}_{AB}$ *coordinate is,*

$$\Delta P_A(\Delta u_{pss}) = C_{pss}\Delta\delta_{AB} + D_{pss}\Delta\dot{\delta}_{AB} \qquad (18)$$

where C_{pss} *and* D_{pss} *are two constants,* $\Delta\dot{\delta}_{AB}$ *denotes the time derivative of* $\Delta\delta_{AB}$ *and* $\Delta u_{pss} = \Delta u_{pss-m}$, Δu_{pss-f} *or* $\Delta u_{pss-pam}$. *If and only if* $D_{pss} > 0$, *the ESS based stabilizer provides positive damping to the tie-line power oscillation. The bigger* D_{pss} *is, the more damping is provided.*

Without loss of generality and affecting the establishment of the above general conclusion, it is assumed that the power oscillation along the transmission line is not affected by any of other system variables, that is, in Eq.(14), (16) and (17)

$$\Delta P_A(\Delta \mathbf{z}) + \Delta P_{A-ess}(\Delta \mathbf{z}) + \Delta P_A(\Delta I_{dc2}) = C_{other}\Delta\delta_{AB} \qquad (19)$$

where C_{other} is a constant. Hence from Eq.(14), (16)-(19) it can be obtained that when one ESS based stabilizer is considered

$$\begin{aligned} \Delta P_A &= (C_{other} + C_{pss})\Delta\delta_{AB} + D_{pss}\Delta\dot{\delta}_{AB} \\ &= C\Delta\delta_{AB} + D_{pss}\Delta\dot{\delta}_{AB} \end{aligned} \qquad (20)$$

Figure 6 shows the linearized $P_A - \delta_{AB}$ curve where (δ_{AB0}, P_{A0}) is the operating point of the power system at steady state. Small-signal oscillation of ΔP_A starts from point 'a' in Figure 6(a) with the operating point moving down. If $D_{pss}\Delta\dot{\delta}_{AB} = 0$ (i.e. $D_{pss} = 0$), the operating point moves down along the line $\Delta P_A = C\Delta\delta_{AB}$. According to the equal area criterion, the operating point stops at point 'f' where the area of triangle 'ade' is equal to that of 'dgf'. This is the case that $\delta_{AB1} - \delta_{AB0} = \delta_{AB0} - \delta_{AB2'}$ and no damping is provided to the power oscillation along the transmission line.

When $D_{pss} > 0$ and the operating point moves down ($\Delta\dot{\delta}_{AB} < 0$), $D_{pss}\Delta\dot{\delta}_{AB} < 0$ will be added on the line $\Delta P_A = C\Delta\delta_{AB}$ as shown by Eq.(20). Hence the operating point should move down below line $\Delta P_A = C\Delta\delta_{AB}$ along the highlighted trajectory shown in Figure 6(a). Obviously the operating point only stops when the area of A_1 is equal to that of A_2 at point 'c' where $\Delta\dot{\delta}_{AB} = 0$ (hence $D_{pss}\Delta\dot{\delta}_{AB} = 0$). Obviously, this is the case that $\delta_{AB1} - \delta_{AB0} > \delta_{AB0} - \delta_{AB2}$ and the power oscillation is damped due to the contribution from $D_{pss}\Delta\dot{\delta}_{AB}$.

Similarly, when $D_{pss} > 0$ and the operating point moves up from point 'c' ($\Delta\dot{\delta}_{AB} > 0$), $D_{pss}\Delta\dot{\delta}_{AB} > 0$ is added on the line $\Delta P_A = C\Delta\delta_{AB}$. Hence the operating point should move up along the highlighted trajectory above line $\Delta P_A = C\Delta\delta_{AB}$ as it is shown in Figure 6(b). The operating point only stops at point 'h' where the area of A_3 is equal to that of A_4 . This leads to that $\delta_{AB3} - \delta_{AB0} < \delta_{AB0} - \delta_{AB2}$, that is, the oscillation is damped because $D_{pss} > 0$. Obviously, the bigger D_{pss} is, the more damping is provided.

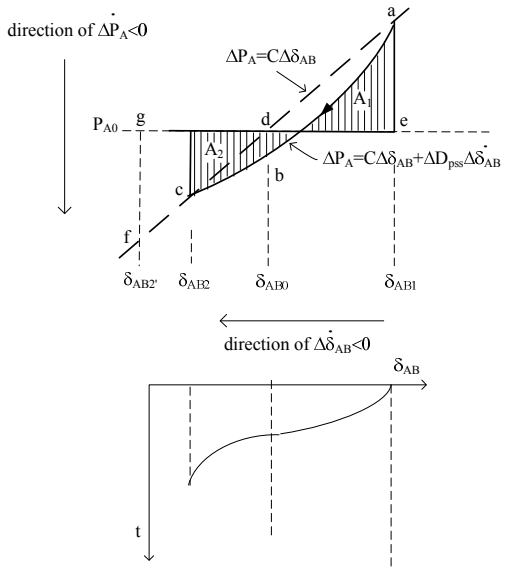

Figure 6(a)

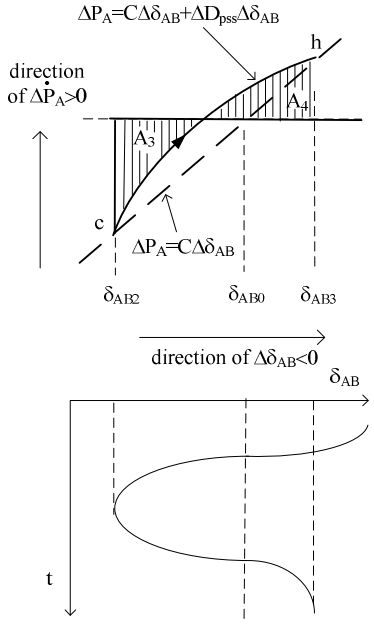

Figure 6(b)

Figure 6 Graphical explanation of the **Conclusion**

Remarks:

1. Eq.(18) is quite similar to the decomposition of electric torque in the damping torque analysis, which has been well

understood and used for studying power system oscillations and control [16]. However Eq.(18) is different because it is not related at all to the concept of damping torque. The conclusion is graphically established only on the movement of power system operating point on the linearized $P_A - \delta_{AB}$ curve. Hence it is general and simple as well as obviously easy to be understood in a multi-machine power system.

2. From Figure 6 it can be seen that as far as the movement of power system operating point is concerned, the direction of $\Delta\dot{\delta}_{AB}$ is that of $\Delta\dot{P}_A$. Hence if the ESS based stabilizer is designed to ensure that

$\Delta P_A(\Delta u_{pss}) = C_{pss}\Delta\delta_{AB} + D_{pss-p}\Delta\dot{P}_A$ and $D_{pss-p} > 0$ (21) its damping effectiveness is guaranteed.

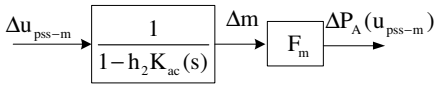

Figure 7 TPVELDM for ESS based reactive power PSS when the PWM is used

Figure 7, 8 and 9 shows the TPVELDM only considering damping contribution from $\Delta P_A(\Delta u_{pss-m})$, $\Delta P_A(\Delta u_{pss-f})$ and $\Delta P_A(\Delta u_{pss-pam})$ respectively. For the ESS based reactive power PSS when the PWM algorithm is used, if Δm in Figure 7 is decomposed in $\Delta\delta_{AB} - \Delta\dot{\delta}_{AB}$ coordinate to be

$$\Delta m = C_{pss-m}'\Delta\delta_{AB} + D_{pss-m}'\Delta\dot{\delta}_{AB}$$

from Figure 7 and Eq.(15) it can have

$$D_{pss} = F_m D_{pss-m}' = \frac{V_A}{X} akV_{dc0}\sin\gamma_0 D_{pss-m}' \quad (22)$$

From Figure 3 and Eq.(22) it can be seen that at a higher loading condition of the tie line, γ_0 and hence D_{pss} is bigger. This means the ESS based reactive power PSS is more effective to suppress the tie line power oscillation at a higher loading condition of the tie line.

In the case of the ESS based active power PSS when the PWM control is implemented, if in Figure 8 the decomposition of Δm, ΔV_{dc} and $\Delta\phi$ in $\Delta\delta_{AB} - \Delta\dot{\delta}_{AB}$ coordinate respectively is

$$\Delta m = C_{pss-fm}\Delta\delta_{AB} + D_{pss-fm}\Delta\dot{\delta}_{AB}$$
$$\Delta V_{dc} = C_{pss-fdc}\Delta\delta_{AB} + D_{pss-fdc}\Delta\dot{\delta}_{AB}$$
$$\Delta\phi = C_{pss-ff}\Delta\delta_{AB} + D_{pss-ff}\Delta\dot{\delta}_{AB}$$

from the above decomposition, Figure 8 and Eq.(15) it can have

$$D_{pss} = F_m D_{pss-fm} + F_{dc} D_{pss-fdc} + F_f D_{pss-ff}$$
$$= \frac{V_A}{X} ak(V_{dc0}\sin\gamma_0 D_{pss-fm} + m_0\sin\gamma_0 D_{pss-fdc} \quad (23)$$
$$+ m_0 V_{dc0}\cos\gamma_0 D_{pss-ff})$$

Because when the loading condition of the tie line increases, $\sin\gamma_0$ increases but $\cos\gamma_0$ decreases in Eq.(23), it is highly possible that the effectiveness of the ESS based active power PSS does not change much. Hence the robustness of the ESS based active power PSS to the variation of tie-line loading conditions is expected to be better than the ESS based reactive power PSS. The same conclusion can be drawn from Figure 9 for the ESS based PSS when the PAM control is used by the DC/AC converter.

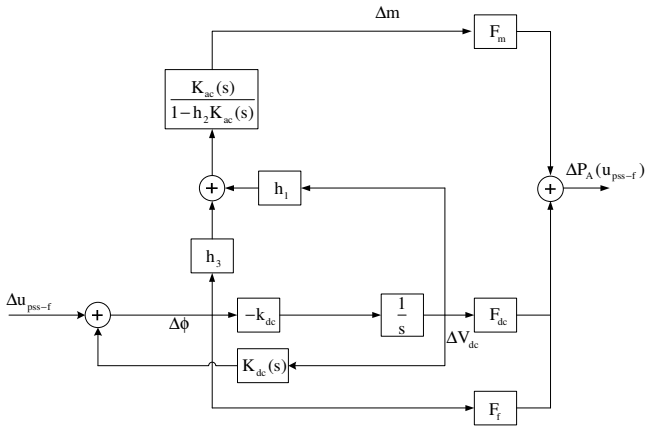

Figure 8 TPVELDM for ESS based active power PSS when the PWM is used

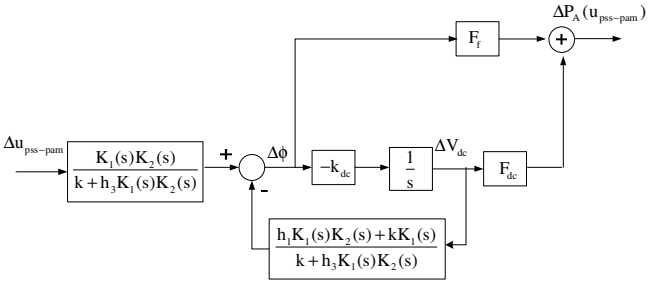

Figure 9 Tie-line power related linearized model for ESS based stabilizer when the PAM is used

From Figure 7, 8 and 9 it can have

$$\Delta P_A(\Delta u_{pss}) = F(s)\Delta u_{pss} \quad (24)$$

where $\Delta u_{pss} = \Delta u_{pss-m}$, Δu_{pss-f} or $\Delta u_{pss-pam}$. According to previous <u>*Remark*</u> 2, an ESS based stabilizer can be designed to satisfy the following equation

$$\Delta P_A(\Delta u_{pss}) == F(s)\Delta u_{pss} = D_{pss-p} s\Delta P_A(D_{pss-p} > 0) \quad (25)$$

to ensure that the tie-line power oscillation is suppressed effectively by the stabilizer. Hence if the local signal of variation of tie-line active power ΔP_A is used as the feedback signal of the stabilizer and the transfer function of stabilizer is constructed by a lead-lag network which is normally used by a conventional PSS (power system stabilizer), it can have

$$\Delta u_{pss} = K_{pss}\frac{sT_w}{1+sT_w}\frac{1+sT_2}{1+sT_1}\frac{1+sT_4}{1+sT_3}\Delta P_A \quad (26)$$

Parameters of the ESS stabilizer can be set at the angular oscillation frequency of the tie line active power, ω_s, to satisfy the following equation

$$F(s)K_{pss}\frac{sT_w}{1+sT_w}\frac{1+sT_2}{1+sT_1}\frac{1+sT_4}{1+sT_3} = D_{pss-mp}s \quad (27)$$

with $s = j\omega_s$. Obviously this method proposed to design the ESS based stabilizer is only based on the TPVELDM. Hence this is a very simple localized method to set parameters of the ESS based stabilizer to suppress inter-area power oscillation. It

does not reply on a linearized model of the whole power system.

IV. AN EXAMPLE POWER SYSTEM INSTALLED WITH A BESS

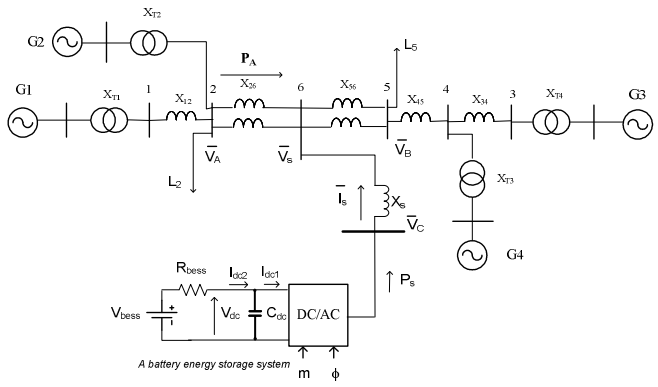

Figure 10 A two-area power system installed with a BESS

Figure 10 shows the configuration of a four-machine two-area power system, where a BESS is installed at node 6 along the tie line connecting two areas of the power system. This is the example power system (without the BESS installed) proposed in [17] for the study of power system inter-area oscillations. It has been used as an example power system to demonstrate the suppression of power system inter-area oscillations [18][19]. Mathematical model of the BESS proposed in [20] is adopted with $I_{dc2} = \dfrac{V_{bess} - V_{dc}}{R_{bess}}$, where the equivalent resistance R_{bess} represents the power loss inside the BESS [20]. Parameters of the example power system are given in [21].

4.1 Design of the BESS based stabilizers

At a steady-state operating condition of the power system when $P_{A0} = 600MW, \delta_{AB0} = 42^0, \gamma_0 = 21^0$, the TPVELDM is established. In order to demonstrate both cases of the PWM and PAM control algorithm, two TPVELDMs of Figure 4 and 5 for the BESS are derived (although in practice the BESS can only adopts one control algorithm). From the TPVELDMs, transfer function $F(s)$ in Eq.(24) is calculated for three types of the BESS based stabilizers

(1) BESS based reactive PSS (PWM);
(2) BESS based reactive power PSS (PWM);
(3) BESS based PAM stabilizer;

Finally three types of the stabilizers are designed by use of the method proposed in the above section according to Eq.(27). In Appendix 3, parameters of the linearized models and the stabilizers set are given.

Figure 11 present the results of non-linear simulation of the example power system with and without the BESS based stabilizers installed when the system is subject to a small disturbance (1% increase of mechanical power input to G4 for 100 ms. at 0.2 second of simulation). Table 1 gives the results of computation of system inter-area oscillation mode.

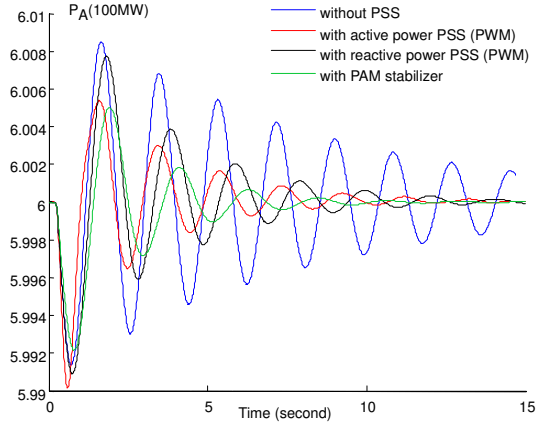

Figure 11 Results of non-linear simulation when the system is subject to a small disturbance

Table 1 Inter-area oscillation mode of the example powers system

Without any BESS based stabilizer	-0.09489 ± j3.411
With BESS based reactive power PSS	-0.3064 ± j3.083
With BESS based active power PSS	-0.3345 ± j3.253
With BESS based PAM stabilizer	-0.4672 ± j2.877

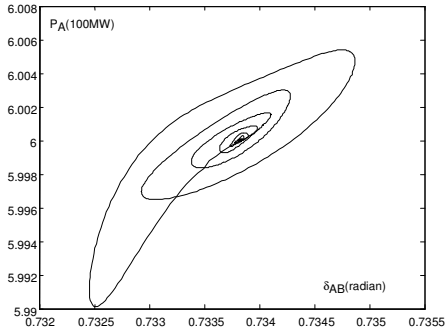

Figure 12 Trajectory of movement of system operating point in the $P_A - \delta_{AB}$ coordinate when the system is with the BESS reactive power PSS

From Figure 11 and Table 1 it can be seen that all three types of BESS based stabilizers are designed successfully by using the proposed method to effectively suppress the inter-area power oscillation. As an example, only the trajectory of movement of system operating point in the $P_A - \delta_{AB}$ coordinate when the power system is subject to the small disturbance and with BESS based reactive power stabilizer installed is given in Figure 12. It is exactly as same as predicted by the analysis shown in Figure 6.

4.2 Robustness of the BESS based stabilizers

Effectiveness of the BESS based stabilizers designed above is tested at a lower tie-line loading condition of the example power system with $P_{A0} = 300MW, \delta_{AB0} = 18^0, \gamma_0 = 14^0$. Figure 13 shows the results of non-linear simulation when the system is subject to the same small disturbance. Table 2 is the results of computation of system inter-area oscillation mode. From Figure 13 and Table 2 it can be seen that at the lower tie-line loading condition, the BESS reactive power PSS cannot effectively suppress the inter-area oscillation any more. The robustness of the BESS based active power PSS and PAM

stabilizer is better than the BESS reactive power PSS, exactly as it is predicted by the analysis in the previous section.

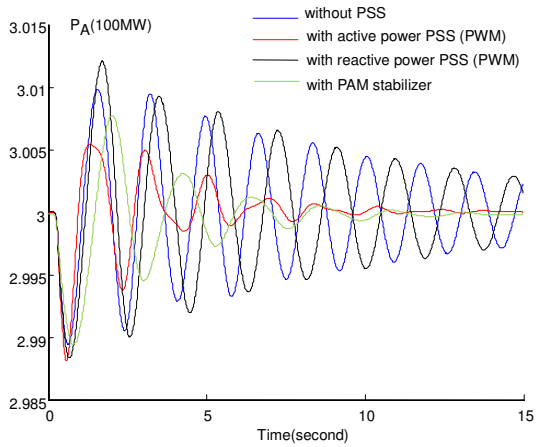

Figure 13 Results of non-linear simulation when the system operates at a lower tie-line loading condition and is subject to a small disturbance

Table 2 Inter-area oscillation mode of the example powers system at a lower tie-line loading condition

Without any BESS based stabilizer	-0.0783 ± j3.648
With BESS based reactive power PSS	-0.1063 ± j3.051
With BESS based active power PSS	-0.3113 ± j3.479
With BESS based PAM stabilizer	-0.3753 ± j3.136

V. Conclusions

In order to investigate how a ESS based stabilizer contributes damping to suppress power system inter-area oscillations, this paper proposes a tie-line power variation related ESS linearized dynamic mode (TPVELDM) which can clearly show the direct contribution from the ESS to the tie-line power variations (oscillations). The paper then establishes a general conclusion about how the tie-line power oscillation is damped as far as the contribution from the ESS is concerned. Based on the TPVELDM proposed and the general conclusion established, a new method is proposed to design the ESS based stabilizers to effectively suppress power system inter-area oscillation. By using the method, the ESS based stabilizer can be designed without the need to be referred to a mathematical model of whole power system. Hence the new method proposed is simple and localized.

Another major contribution of the paper is the examination of the robustness of the ESS based stabilizers to the variations of tie-line loading conditions. Analysis indicates that the ESS based stabilizers via regulating active power exchange between the ESS and the power system, i.e., ESS active power PSS and ESS PAM PSS, is more robust than the ESS based reactive power PSS which controls directly the reactive power exchange between the ESS and the power system. This is because ESS active power PSS and ESS PAM stabilizer suppress the inter-area power oscillation directly by absorbing active power from or injecting it to the power system when they "see" the excess or lack of active power delivered along the tie line. Their capability to damp the tie-line power oscillation is not affected much by the tie-line loading conditions. The ESS reactive power PSS regulates its exchange of reactive power with the tie line to affect indirectly the variation of active power delivered along the tie line. At a higher tie-line loading condition, regulation of reactive power exchange is related more closely with the variation of tie-line active power. Hence the ESS based reactive power PSS is more effective in damping the inter-area power oscillations.

In the paper, an example power system installed with a BESS is presented. Results of numerical computation and non-linear simulation demonstrate and confirm all analytical conclusions obtained and effectiveness of the method proposed in the paper to design the ESS based stabilizers.

VI. References

[1] P. F. Ribeiro, B. K. Johnson, M. L. Crow, A. Arsoy and Y. Liu, "Energy storage systems for advanced power applications", IEEE Proc., Vol. 89, No. 12, .2001, pp1744-1756

[2] C. S. Hsu and W. J. Lee, "Superconducting magnetic energy storage for power system applications", IEEE Trans. on Industry Applications, Vol.29, No.5, 1993, pp990 - 996

[3] J. D. Rogers, H. J. Boenig, J. C. Bronson, D. B. Colyer, W. V. Hassenzahl, R. D. Turner and R. I. Schermer, "30-MJ superconducting magnetic energy storage (SMES) unit for stabilizing an electric transmission systems", IEEE Trans. on Magnetics, Vol.15, No.1, 1979, pp820-823

[4] Y. Mitani, K. Tauji and Y. Murakami, "Application of superconducting magnet energy storage to improve power system dynamic performance", IEEE Trans. on Power Systems, Vol.3, No.4, 1988, pp1418-1425

[5] A. H. M. A. Rahim and A. M. Mohammad, "Improvement of synchronous generator damping through superconducting magnetic energy storage systems", IEEE Trans. on Energy Conversion, Vol.9, No.4, 1994, pp736-742

[6] J. B. Simo and I. Kamwa, "Exploratory assessment of the dynamic behaviour of multimachine system stabilized by a SMES unit", IEEE Trans. on Power Systems, Vol.10, No.3, 1995, pp1566-1571

[7] M. W. Tsang and D. Sutanto, "Power system stabiliser using energy storage", IEEE, PES Winter Meeting, Vol.2, 2000, pp1354 - 1359

[8] S. Arabi and P. Kundur, "Stability modelling of storage devices in FACTS applications", IEEE PES Summer Meeting, Vol.2, 2001, pp767 - 771

[9] Z Yang, C Shen, L Zhang, M Crow and S Atcitty, "Integration of a StatCom and a battery energy storage", IEEE Trans. Power Systems, Vol. 16, No.2, pp254-260, May, 2001

[10] B. Bhargava and G. Dishaw, "Application of an energy source power system stabilizer on the 10 MW battery energy storage system at Chino substation", IEEE Trans. on Power Systems, Vol.13, No.1, 1998, pp145 – 151

[11] "Modeling of power electronics equipment (FACTS) in load flow and stability programs", CIGRE T F 38-01-08, 1998

[12] S Samineni, B. K. Johnson, H. L. Hess and J. D. Law, "Modelling and analysis of a flywheel energy storage system with a power converter interface", Prof. of IPST, 2003, New Orleans, USA, pp1-6

[13] J. M. Carrasco, L. G. Franquelo, etc., "Power electronic systems for the grid integration of renewable energy sources: a survey", IEEE Trans. on Industrial Electronics, Vol. 53, No.4, 2006, pp1002-1016

[14]M Kazmierkowski and L Malesani, "Current control techniques for three-phase voltage-source PWM converters: a Survey", IEEE Trans. on Industrial Electronics, Vol. 45, No.5, pp691-703, Oct. 1998

[15] L Zhang, L Harnefors and H Nee, "Power-synchronization control of grid-connected volrafe-source converters", IEEE Trans. on Power Systems, Vol.25, No.2, pp809-820, May 2010

[16] E.V. Larsen and D.A. Swann, "Applying power system stabilizers Part I-III", IEEE Trans. Power Appar. Syst., Vol. 100, No. 6, 1981, pp3017-3046

[17] M. Klein, G. J. Roger and P. Kundur, "A fundamental study of inter-area oscillations in power systems", IEEE Trans. Power Syst., Vol.6, No. 3, 1991, pp914-921

[18] X. Yang, and A. Feliachi, "Stabilization of inter-area oscillation modes through excitation systems", IEEE Trans. Power Syst., Vol.9, No.1, 1994, pp494-502

[19] D.Z. Fang, Yang Xiaodong, Song Wennan and H.F.Wang, 'Oscillation transient energy function and its application to design a TCSC fuzzy logic damping controller to suppress power system inter-area mode oscillations', IEE Proc. Part C, No.2, 2003

[20] Chen Shen, Zhiping Yang, M. L. Crow and S. Atcitty, "Control of STATCOM with energy storage device", Power Engineering Society Winter Meeting, 2000. IEEE, Volume 4, 23-27 Jan. 2000 pp2722 – 2728.
[21] P Kunder, Power system stability and control, McGraw-Hill, 1994

Acknowledgement

The authors would like to acknowledge the support of the EPSRC UK-China joint research consortium (EP/F061242/1), the science bridge award (EP/G042594/1), UK, Jiangsu Power Company, China, and the Fund of Best Post-Graduate Students of Southeast University, China. Prof. Haifeng Wang is a member of the international innovation team of superconducting technology for electrical engineering at the Institute of Electrical Engineering, Beijing, China, sponsored by the Chinese Academy of Sciences, China.

APPENDIX 1

From Figure 1 and 2 it can have $\bar{V}_c = jX_s\bar{I}_s + \bar{V}_s$ which can give

$$I_{sd} = \frac{V_c \sin\phi}{X_s}, I_{sq} = \frac{V_s - V_c\cos\phi}{X_s} \quad \text{(A-1)}$$

There is no exchange of active power between the ESS and power system at steady-state operation, i.e., $\phi_0 = 0$. Hence $I_{sd0} = 0$ and

$$\Delta I_{sd} = \Delta\frac{mkV_{dc}\sin\phi}{X_s} = \frac{k\sin\phi_0}{X_s}(V_{dc0}\Delta m + m_0\Delta V_{dc})$$
$$+\frac{m_0kV_{dc0}\cos\phi_0}{X_s}\Delta\phi = \frac{m_0kV_{dc0}}{X_s}\Delta\phi = \frac{V_{c0}}{X_s}\Delta\phi$$
$$I_{sq0} = \frac{V_{s0} - V_{c0}}{X_s}$$

By using the above equation, linearization of Eq.(2) can be obtained to be

$$\Delta\dot{V}_{dc} = \frac{1}{C_{dc}}[-I_{sd0}(k\cos\phi_0\Delta m - m_0k\sin\phi_0\Delta\phi) - I_{sq0}(k\sin\phi_0\Delta m + m_0k\cos\phi_0\Delta\phi)$$
$$-m_0k\cos\phi_0\Delta I_{sd} - m_0k\sin\phi_0\Delta I_{sq} + \Delta I_{dc2})$$
$$= \frac{1}{C_{dc}}(-I_{sq0}m_0k\Delta\phi - m_0k\frac{V_{c0}}{X_s}\Delta\phi + \Delta I_{dc2}) = \frac{1}{C_{dc}}(-m_0k\frac{V_{s0}}{X_s}\Delta\phi + \Delta I_{dc2})$$

Appendix 2

From Figure 1 and Eq.(11) it can have

$$\bar{V}_A = jX(I_{Asx} + jI_{Asy}) + \bar{V}_a = -XI_{Asy} + V_a\cos\delta' + jXI_{Asx} + jV_a\sin\delta' \quad \text{(A-2)}$$

where subscript x and y denotes the x and y component of the corresponding variable respectively in the x-y coordinate of the power system as shown by Figure 3. From Eq.(A-2) it can be obtained

$$I_{Asx} = -\frac{V_a\sin\delta'}{X}, I_{Asy} = \frac{V_a\cos\delta' - V_A}{X} \quad \text{(A-3)}$$

Because

$$\bar{V}_A = jX_{As}\bar{I}_{As} + \bar{V}_s = jX_{As}(I_{Asx} + jI_{Asy}) - X_{As}I_{AsY} + V_{sx} + jV_{sy} \quad \text{(A-4)}$$

it can be obtained from Eq.(A-3) and (A-4) that

$$V_{sx} = V_A + X_{As}I_{Asy} = V_A + X_{As}\frac{V_a\cos\delta' - V_A}{X} = \frac{X_{As}}{X}V_a\cos\delta' + (\frac{X - X_{As}}{X})V_A$$
$$= \frac{X_{As}}{X}(bV_B\cos\delta_{AB} + akmV_{dc}\cos\gamma) + (\frac{X - X_{As}}{X})V_A$$
$$V_{sy} = -X_{As}I_{Asx} = X_{As}\frac{V_a\sin\delta'}{X} = \frac{X_{As}}{X}(bV_B\sin\delta_{AB} + akmV_{dc}\sin\gamma) \quad \text{(A-5)}$$

Because

$$\bar{V}_s = V_{sx} + jV_{sx} = -jX_s\bar{I}_s + \bar{V}_c = -jX_s(I_{sx} + jI_{sy}) + V_c\cos\gamma + jV_c\sin\gamma \quad \text{(A-6)}$$

it can have

$$I_{sx} = \frac{V_c\sin\gamma - V_{sy}}{X_s}, I_{sy} = \frac{V_{sx} - V_c\cos\gamma}{X_s} \quad \text{(A-7)}$$

Linearization of Eq.(A-5) is

$$\Delta V_{sx} = a_{1x}'\Delta V_{dc} + a_{2x}'\Delta m + a_{3x}'\Delta\gamma + a_{4x}'\Delta\delta_{AB} + a_{5x}'\Delta V_A + a_{6x}'\Delta V_B$$
$$\Delta V_{sy} = a_{1y}'\Delta V_{dc} + a_{2y}'\Delta m + a_{3y}'\Delta\gamma + a_{4y}'\Delta\delta_{AB} + a_{5y}'\Delta V_A + a_{6y}'\Delta V_B \quad \text{(A-8)}$$

Because the modulation phase, ϕ, is the angle between $\bar{V}_s$ and $\bar{V}_c$, as given in Eq.(1), that is

$$\gamma = \phi + \arctan^{-1}\frac{V_{sy}}{V_{sx}} \quad \text{(A-9)}$$

from Eq.(A-8) and (A-9) it can have

$$\Delta\gamma = \Delta\phi + a_1'\Delta V_{dc} + a_2'\Delta m + a_3'\Delta\gamma + a_4'\Delta\delta_{AB} + a_5'\Delta V_A + a_6'\Delta V_B \quad \text{(A-10)}$$

That gives

$$\Delta\gamma = a\Delta\phi + a_1\Delta V_{dc} + a_2\Delta m + a_4\Delta\delta_{AB} + a_5\Delta V_A + a_6\Delta V_B \quad \text{(A-11)}$$

By substituting Eq.(A-12) into (A-8) and (A-9) it can be obtained that

$$\Delta V_{sx} = a_{1x}\Delta V_{dc} + a_{2x}\Delta m + a_{3x}\Delta\phi + a_{4x}\Delta\delta_{AB} + a_{5x}\Delta V_A + a_{6x}\Delta V_B$$
$$\Delta V_{sy} = a_{1y}\Delta V_{dc} + a_{2y}\Delta m + a_{3y}\Delta\phi + a_{4y}\Delta\delta_{AB} + a_{5y}\Delta V_A + a_{6y}\Delta V_B \quad \text{(A-12)}$$

From Eq.(A-12) it can have

$$\Delta V_s = h_1\Delta V_{dc} + h_2\Delta m + h_3\Delta\phi + h_4\Delta\delta_{AB} + h_5\Delta V_A + h_6\Delta V_B \quad \text{(A-13)}$$

Appendix 3 Design of ESS based stabilizers

For the BESS, it can have

$$\Delta I_{dc2} = -\frac{1}{R_{bess}}\Delta V_{dc}$$

Hence block $\frac{1}{s}$ in Figure 4 and 5 should be replaced by $\frac{C_{dc}R_{bess}}{C_{dc}R_{bess}s + 1}$ where $R_{bess} = 0.01$

1. Parameters of the TPVELDM of Figure 4 when the PWM is implemented

$$K_{ac}(s) = 0.1 + \frac{0.85}{s}; K_{dc}(s) = 0.2 + \frac{2}{s};$$
$$h_1 = 0.0891; h_2 = -0.4508; h_3 = 0.0; h_4 = 0.0055; h_5 = 0.9016; h_6 = 0.0062;$$
$$k_{dc} = 97.7244; F_m = -2.7360; F_{dc} = -0.5409; F_f = 97.0570$$

2. $F(j\omega_s)$ ($\omega_s = 3.411$) for the design of the BESS active power PSS

$$F(j\omega_s) = 69.87 + j9.077 = 70.46\angle 7.4^0$$

Parameters of the BESS active power PSS

$$K_{pss} = 0.0001898; T_1 = 3.309s.; T_2 = 0.4s.; T_3 = 3.309s.; T_4 = 0.4s.$$

3. $F(j\omega_s)$ ($\omega_s = 3.411$) for the design of the BESS active power PSS

$$F(j\omega_s) = -2.403 + j0.5417 = 2.464\angle 167.39^0$$

Parameters of the BESS reactive power PSS

$$K_{pss} = 0.05414; T_1 = 0.07918s.; T_2 = 0.4s.; T_3 = 0.07918s.; T_4 = 0.4s.$$

4. Parameters of the TPVELDM of Figure 5 when the PAM is implemented

$$K_1(s) = 0.1 + \frac{0.5}{s}; K_2(s) = \frac{1}{s};$$
$$h_1 = 0.4618; h_3 = 0.0; h_4 = 0.0295; h_5 = 0.4753; h_6 = 0.0373;$$
$$k_{dc} = 94.0499; F_{dc} = -2.8571; F_f = 87.1842$$

5. $F(j\omega_s)$ ($\omega_s = 3.411$) for the design of the BESS PAM stabilizer

$$F(j\omega_s) = 3.308 + j3.017 = 4.478\angle 42.4^0$$

Parameters of the BESS PAM stabilizer

$$K_{pss} = 0.05951; T_1 = 1.328s.; T_2 = 0.4s.; T_3 = 1.328s.; T_4 = 0.4s.$$

BIOGRAPHIES

Wendy DU is with the Southeast University, Nanjing, China and working as a Research Fellow at the Queen's University of Belfast. Her main research interests are power system stability analysis and control, including energy storage systems, FACTS and renewable power generation. Her contact e-mail address is ddwenjuan@qub.ac.uk